Appl Phys A (2012) 106:501–506
DOI 10.1007/s00339-011-6720-6

Applied Physics A
Materials Science & Processing

RAPID COMMUNICATION

Investigation of Raman and photoluminescence studies of reduced graphene oxide sheets

Karthikeyan Krishnamoorthy · Murugan Veerapandian · Rajneesh Mohan · Sang-Jae Kim

Received: 12 September 2011 / Accepted: 1 December 2011 / Published online: 15 December 2011

Abstract In this paper, we are investigating the Raman and photoluminescence properties of reduced graphene oxide sheets (rGO). Moreover, graphene oxide (GO) sheets are synthesized using Hummer's method and further reduced into graphene sheets using D-galactose. Both GO and rGO are characterized by UV-vis spectroscopy, X-ray diffraction (XRD), X-ray photoelectron spectroscopy (XPS) and Thermogravimetric (TGA) analysis. Raman analysis of rGO shows the restoration of graphitic domains in GO after reduction. The photoluminescence of rGO showed emission in the UV region which is blue shifted along with luminescent quenching as compared to GO. This blue shift and quenching in photoluminescence arises due to the newly formed crystalline sp^2 clusters in rGO which created percolation pathways between the sp^2 clusters already present.

1 Introduction

Graphene is a single sheet of carbon atoms tightly packed into a two-dimensional (2D) honeycomb lattice [1]. Graphene sheets are of significance in fundamental and applied science due to their exceptional electronic, tunable band gap, high mobility, mechanical, and thermal properties [2, 3]. These unique properties of graphene are promising for applications in various fields such as nanoelectronics, nanocomposites, gas sensors, batteries and hydrogen storage [4, 5]. In this regard, an outstanding challenge is to integrate photonic and band-gap manipulation. Since graphene has no band gap, photoluminescence has is not expected from relaxed charge carriers [6], but it can be made luminescent mainly by two ways viz. (i) by cutting into ribbons and quantum dots [7] and (ii) by physical or chemical treatments [8]. Previous report on graphene nanoribbons with various band gaps exhibited no photoluminescence [9]. Some of the reports show that graphene can be made luminescent by oxygen plasma treatment [10]. Similarly, chemically synthesized graphene oxide (GO) exhibits a broad photoluminescence where the electronic structure has been modified [11]. GO is basically insulating and highly disordered compared to the crystalline graphene. But the availability of various oxygen-containing functional groups with both sp^2 and sp^3 carbon sites made them attractive towards synthesis of large scale production of graphene by suitable reduction kinetics. The band gap of GO can be tunable by varying the oxidation level [12]. Even though GO is formed from the oxidation of graphite, still it have some sp^2 carbon atoms in its structure. The density-functional studies on GO show the presence of graphitic domains in the GO which produce quantum confinement effects in GO [13]. The property of graphene can be altered by suitable reduction process of GO by controlling the fractions of sp^2 to sp^3 clusters and resulting in transition from insulator to semiconductor and to a metal [14]. Therefore, it is expected that the optical properties of the graphene sheets can be tuned by the reducing GO into reduced graphene oxide sheets (rGO) by altering the sp^2 to sp^3 ratio.

K. Krishnamoorthy · S.-J. Kim (✉)
Nano Materials and System Lab, Department of Mechanical Engineering, Jeju National University, Jeju 690-756, South Korea
e-mail: kimsangj@jejunu.ac.kr
Fax: +82-64-7563886

M. Veerapandian
College of BioNano Technology, Kyungwon University, Gyeonggi-Do 461-701, South Korea

R. Mohan · S.-J. Kim
Department of Mechatronics Engineering and Research Institute of Advanced Technology, Jeju National University, Jeju 690-756, South Korea

In these aspects, we are investigating the optical properties of reduced graphene oxide sheets using Raman and photoluminescence spectroscopy. The GO nanosheets are synthesized according to Hummer's method and are successfully reduced using D-galactose into rGO nanosheets. The use of D-galactose is due to its non-toxicity over the conventional chemical reducing agents such as hydrazine and hydrazine hydrate and also in order to avoid agglomeration of graphene sheets [15, 16]. Both GO and rGO are characterized using physico-chemical techniques and their photoluminescence properties before and after reduction are discussed in detail.

2 Experimental

2.1 Synthesis of graphene oxide

GO was synthesized by harsh oxidation of graphite powder using the modified Hummer's method which results in a brownish colloidal suspension [17]. Briefly, the expandable graphite powders (2 g) were stirred in 98% H_2SO_4 (35 mL) for 2 h. Subsequently, $KMnO_4$ (6 g) was gradually added to the above solution while keeping the temperature less than 20°C. The mixture was then stirred at 35°C for 2 hours. The resulting solution was diluted by adding 90 mL of water under vigorous stirring and a dark brown suspension was obtained. The suspension was further treated by adding 30% H_2O_2 solution (10 mL) and 150 mL of distilled water. The resulting graphite oxide suspension was washed by repeated centrifugation, first with 5% HCl aqueous solution and then with distilled water until the pH of the solution becomes neutral. The GO nanostructures were obtained by adding 160 mL of water to the resulting precipitate and sonicated well to attain a uniform suspension of GO.

2.2 Synthesis of reduced graphene oxide

The rGO was synthesized from GO using an eco friendly method by employing galactose as a reducing agent. Briefly, galactose (0.4 g) is gradually added to the aqueous solution of GO (0.5 mg/mL) and is treated by constant stirring for 30 min, resulting in a color change from brown to black. Then, 0.2 mL of ammonia is added to the solution and it is allowed to heat at 70°C for 1 hour. Finally, the black precipitate of rGO obtained was centrifuged at an rpm of 5000 and washed three times with deionized water.

2.3 Characterization

The UV-vis spectroscopy was performed using Hewlett Packard HP-8453 spectrophotometer. The phase purity and crystallinity of the GO and rGO were determined by X-ray diffraction (XRD) recorded on X-ray diffractometer system (D/MAX 2200H, Bede 200, Rigagu Instruments C). The X-ray photoelectron spectroscopy (XPS) measurements were carried out on ESCA 2000 VG Microtech systems. The Raman spectra were recorded with a RENISHAW (M005-141) Raman system with laser frequency of 514 nm as excitation source. The laser spot size was 1 μm, and the power at the sample was below 10 mW, in order to avoid laser-induced heating. Thermogravimetric analysis (TGA) was carried out using Perkin-Elmer instrument. Photoluminescence (PL) spectra of GO and rGO were measured by Cary Eclipse Fluorescence Spectrophotometer.

3 Results and discussion

In this work, GO was synthesized according to the modified Hummer's method and their characterization were discussed in detail in our previous report [17]. The reduction reaction of graphene oxide into graphene sheets was monitored by the color change from brown into black as shown in the inset of Fig. 1(a) followed by the UV-vis spectroscopy. The black color of the rGO material suggested the re-graphitization of the exfoliated GO by the removal of oxygenated functional groups. Figure 1(a) depicts the UV-vis spectra of the GO, showing a sharp absorption peak at 226 nm, which is attributed to the π–π^* of the C–C aromatic rings [18]. After the reduction of GO, the absorption peak was red shifted towards into 272 nm due to the formation of rGO. This is in agreement with previous reports on rGO [19]. The significant red shift in rGO is due to the increased electron concentration, structural ordering and consistent with the restoration of sp^2 carbon atoms [20].

Figure 1(b) shows the XRD pattern of graphite, GO and rGO, respectively. The diffraction peak of pure graphite is found around 26° [21]. After successful oxidation, the diffraction peak of GO shifted towards $2\theta = 10°$ which is mainly due to the oxidation of graphite and the corresponding interlayer spacing was 0.85 nm [22]. The reduction of graphene oxide into rGO is also confirmed by the XRD pattern of rGO which shows a broad diffraction peak at $2\theta = 26°$ corresponding to the interlayer spacing of 0.35 nm. The complete disappearance of a peak at $2\theta = 10°$ of the GO and the formation of new broad peak at $2\theta = 26°$ further supports that the graphene oxide is completely reduced into rGO [16]. Figure 2 shows the TEM image of the reduced graphene oxide showing sheet-like morphology which is transparent and wrinkled at the edges.

The removal of oxygenated functional groups from GO after reduction into graphene is studied by XPS technique as shown in Fig. 3. XPS of GO exhibits the following peaks: at 284.8, 285.55, 286.8 and 288.65 eV, corresponding to the C–C in the aromatic rings, hydroxyl, epoxyl and carbonyl

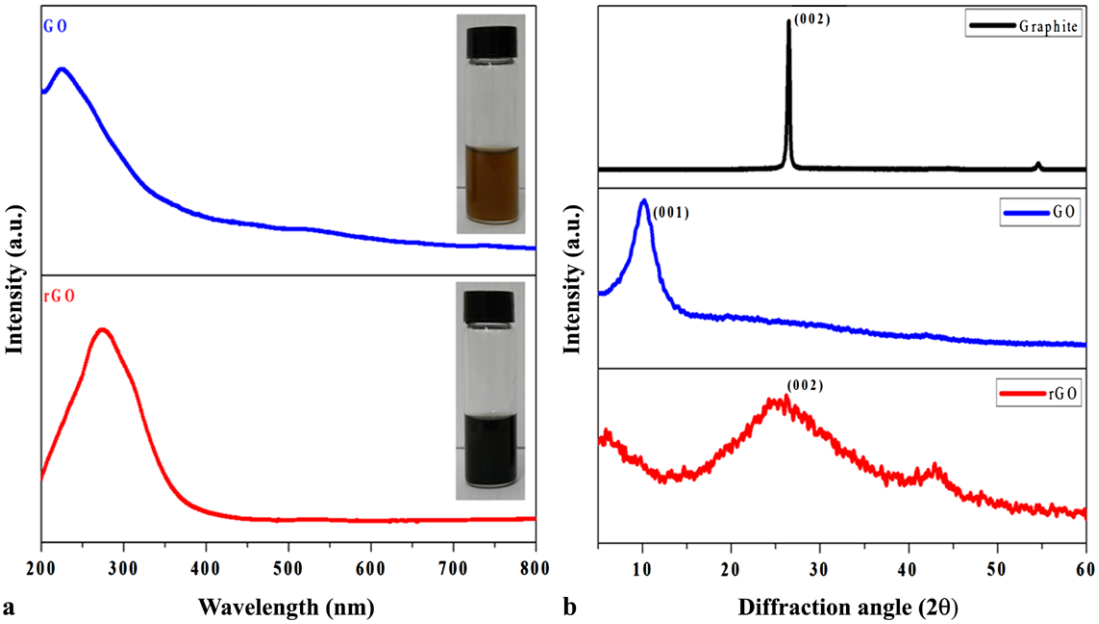

Fig. 1 (**a**) UV-vis spectra of GO and rGO. The photographs correspond to the water dispersed GO and rGO. (**b**) XRD pattern of graphite, GO and rGO

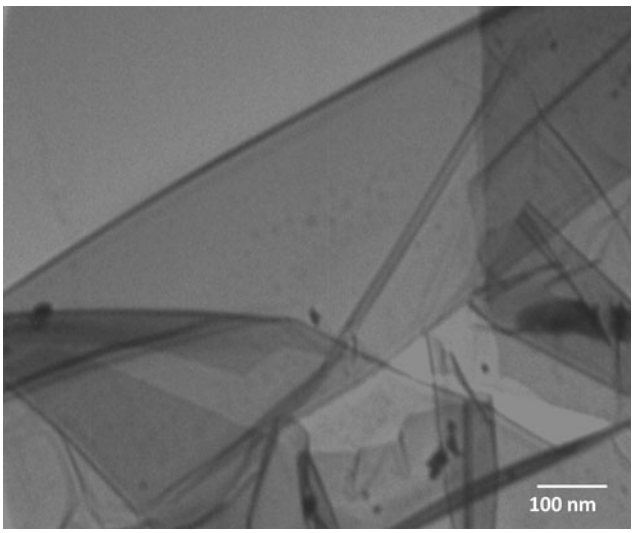

Fig. 2 TEM image of synthesized rGO showing sheet-like morphology

groups, respectively [24]. During the reduction reaction, the hydroxyl, carbonyl and epoxyl groups in GO were effectively reduced by D-galactose. In the XPS of rGO, only the peak due to the C–C bond at 284.8 eV is preserved and all the intensities of other peaks related to the bonding between the carbon and the oxygen such as hydroxyl, epoxyl and carbonyl are relatively decreased, strongly suggests the removal of the oxygenated functional groups [23].

Raman spectroscopy has been a major experimental technique to study the bonding nature of various carbon materials. In order to further characterize the reduction reaction and to study the nature of sp^2 domains, Raman analyses were performed on the reduced GO and compared with GO as shown in Fig. 4(a) and 4(b). The Raman spectra of graphite show a strong G peak at 1570 cm^{-1} due to the first order scattering of E2g mode [25]. The Raman spectra of graphene oxide show that the G peak is shifted towards 1595.89 cm^{-1} due to the oxygenation of graphite [26]. In addition to this, a broadened D peak at 1350 cm^{-1} also appeared due to the reduction in size of *in plane* sp^2 domains in graphite induced by the creation of defects, vacancies and distortions of the sp^2 domains after complete oxidation [27].

After reduction of graphene oxide, the G peak is shifted towards lower wave number (1591.41 cm^{-1}) compared to that of GO, which agrees with the previous reports [28]. This shift was attributed to the recovery of hexagonal network of carbon atoms with defects. The D peak intensity is increased in rGO compared to that of GO suggesting that the reduction process modified the structure of GO with defects [29]. However the decrease in FWHM of the D peak in rGO is due to the increase in average size of the sp^2 clusters [30]. The $I_{(D)}/I_{(G)}$ ratio are used to evaluate the average size of the sp^2 cluster in the graphene materials. The corresponding $I_{(D)}/I_{(G)}$ ratio of GO and rGO are measured as 0.8 nm and 0.9 nm, respectively. In order to determine the average size of the sp^2 clusters in GO and rGO, we employed the Tuinstra and Koenig relation, which relates the ratio of D and G peak into the crystallite size as follows [31]:

$$I_{(D)}/I_{(G)} = C(\lambda)/L_a, \quad (1)$$

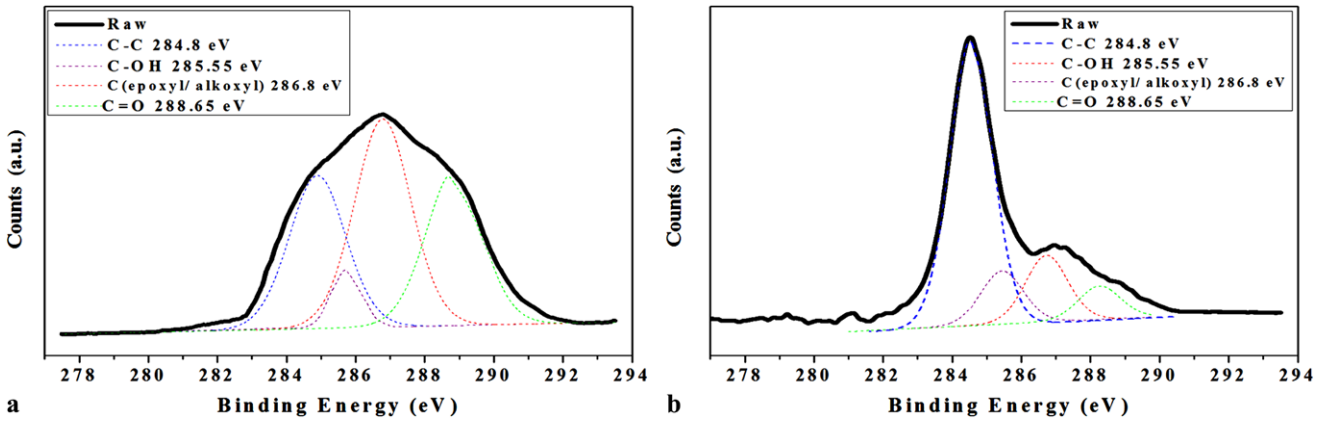

Fig. 3 X-ray photoelectron spectra of (**a**) GO and (**b**) rGO

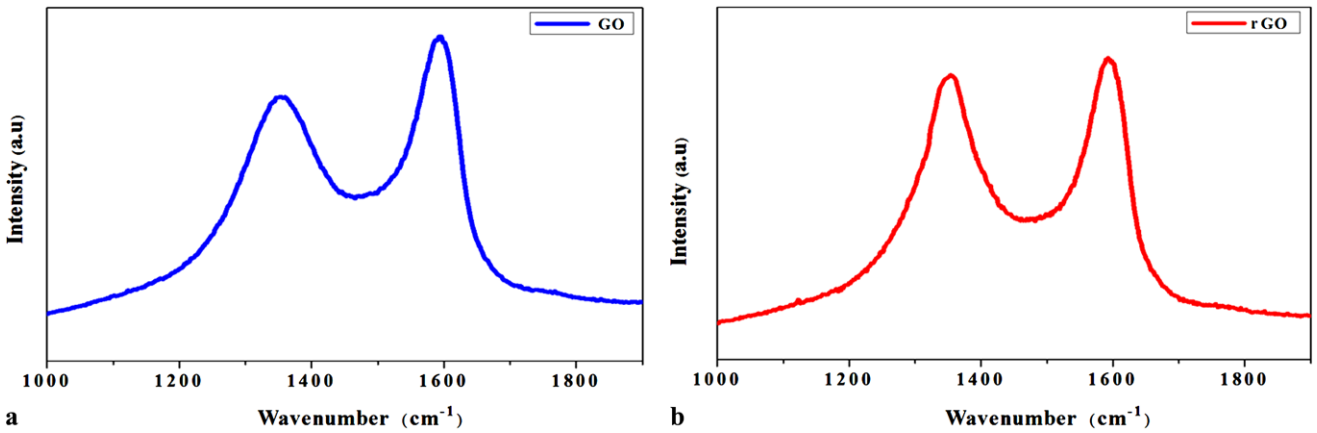

Fig. 4 Raman spectra of (**a**) GO and (**b**) rGO

where $I_{(D)}$ is the intensity of the D peak, $I_{(G)}$ is the intensity of the G peak, $C(\lambda)$ is the wavelength dependent prefactor and L_a is the average crystallite size of sp^2 domains. The average sizes of the sp^2 clusters in GO and rGO were found as 5.28 and 4.57 nm, respectively. The decrease in average size of sp^2 clusters is due to the formation of new sp^2 clusters which are smaller in size compared to the ones present in GO before reduction [15, 26].

The thermal stability of the rGO is studied using thermo gravimetric analysis and compared with the GO and the precursor graphite as shown in Fig. 5. The TGA analysis of graphite shows the high thermal stability of graphite even at 1000°C. Since GO is thermally unstable, it starts losing the mass from 100°C due to the removal of moisture content. The major mass loss occurs at 200°C due to the removal of oxygen-containing functional groups such as CO, CO_2 and H_2O vapors. In case of rGO, already the oxygen-containing functional groups were removed during the reduction process, yielding a better thermal stability than the GO. The TGA of rGO shows the removal of water content at 100°C. This is well in agreement with the previous report on reduced graphene sheets [26]. All these results suggest that graphene oxide is reduced into graphene sheets by using D-galactose as a reducing agent.

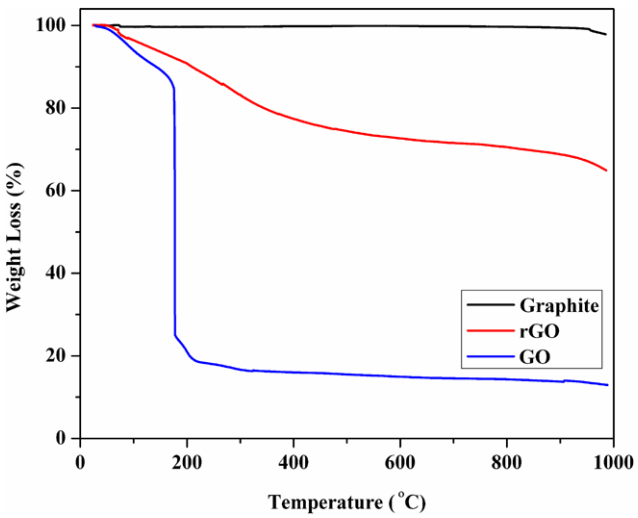

Fig. 5 Thermogravimetric analysis of graphite, GO and rGO

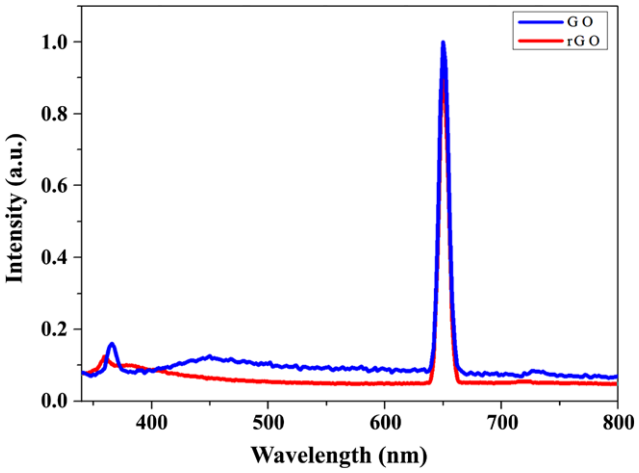

Fig. 6 Photoluminescence spectra of GO and rGO

The study on the optical properties of graphene sheets is an important aspect for its application in photonics [32]. The oxidation of graphite causes the formation of graphitic islands in GO which produces a disruption of the π-network and thus opens up a band gap in the electronic structure [33]. Figure 6 shows the photoluminescence spectra of GO and rGO nanosheets recorded using an excitation wavelength of 325 nm. The PL spectrum of GO shows a sharp emission peak in the near ultraviolet UV region at 365 nm corresponding to the band emission of GO. The unusual strong intensity at 650 nm is not due to the GO sample but due to the overlap of the second-order emissions associated to the excitation wavelength [14]. The UV emission in GO is due to the oxidation of graphite which produce various sizes of crystalline graphitic sp^2 clusters surrounded by amorphous sp^3 matrix in GO which act as a high tunnel barrier resulting in the creation of band gap in GO. PL response of graphene oxide in the low energy region has been reported earlier recently [34]. The PL spectrum of rGO nanosheets also exhibits a sharp emission at 650 nm due to the overlap of the second-order emissions as similar in GO. This second-order emission was verified by using a range of excitation wavelength (325, 400 and 500 nm). The near band emission is quenched and blue shifted (359 nm) after the reduction process. The intensity of the PL emission of rGO is reduced by half compared to GO after the reduction process shows the quenching in PL emission. Although the mechanism of light emission from rGO still unclear and remains unexplored, the quenching of PL quantum yields is possibly due to the following reason. The quenching of PL in rGO is due to the removal of functional groups which is due to the restoration of more number of sp^2 clusters in the graphene sheet after reduction. The newly formed sp^2 clusters in rGO can provide percolation pathways between sp^2 clusters already present. Thus, the reduction of GO results in formation of zero gap regions in the rGO sheets with some of the functional groups remains still unreduced even after the reduction process. This ensures that the ratio of the zero gap sp^2 clusters is comparatively high enough to the sp^3 clusters in the rGO sheets resulting in quenching of photoluminescence due to weak carrier confinement. This is supported by our XPS spectra [Fig. 3] and Raman spectra [Fig. 4] of the rGO sheets. Hence with our results, we can believe that the photoluminescence in GO and rGO depends on the size or length scale of the graphitic regions (sp^2 domains) and the oxidized regions (sp^3 domains). In this regard, it is much needed to investigate more the levels of oxidized and unoxidized region in both GO and rGO since no straightforward relationship exists.

4 Conclusions

In conclusion, rGO sheets are synthesized from GO using D-galactose and are characterized using physical and chemical methods. The studies on XPS show the existence of small fractions of oxygenated functional groups in the rGO sheets even after reduction. Raman analysis shows the formation of new sp^2 clusters in rGO sheets. Moreover, the obtained rGO sheets exhibited quenching in PL emission spectra and are blue shifted due to increased sp^2 clusters after reduction.

Acknowledgements This research was supported by National Research Foundation of Korea Grant under Contract Nos. 2009-0087091 and 2011-0015829, through the Human Resource Training Project for Regional Innovation. A part of this work was carried out at the Research Instrument Center (RIC), Jeju National University, Jeju, Republic of Korea.

References

1. K.S. Novoselov, A.K. Geim, S.V. Morozov, D. Jiang, M.I. Katsnelson, I.V. Grigorieva, S.V. Dubonos, A.A. Firsov, Nature **438**, 197 (2005)
2. S.V. Morozov, K.S. Novoselov, M.I. Katsnelson, F. Schedin, D.C. Elias, J.A. Jaszczak, A.K. Geim, Phys. Rev. Lett. **100**, 016602 (2008)
3. V. Gunasekaran, S.-J. Kim, Curr. Appl. Phys. (2011). doi:10.1016/j.cap.2011.03.030
4. G. Lu, L.E. Ocola, J. Chen, Appl. Phys. Lett. **94**, 083111 (2009)
5. D.R. Lenskia, M.S. Fuhrer, J. Appl. Phys. **110**, 013720 (2011)
6. C.H. Lui, K.F. Mak, J. Shan, T.F. Heinz, Phys. Rev. Lett. **105**, 127404 (2010)
7. X. Li, X. Wang, L. Zhang, S. Lee, H. Dai, Science **319**, 1229 (2008)
8. S. Park, R.S. Ruoff, Nat. Nanotechnol. **4**, 217 (2009)
9. M.Y. Han, B. Ozyilmaz, Y. Zhang, P. Kim, Phys. Rev. Lett. **98**, 206805 (2007)
10. T. Gokus, R.R. Nair, A. Bonetti, M. Bohmler, A. Lombardo, K.S. Novoselov, A.K. Geim, A.C. Ferrari, A. Hartschuh, ACS Nano **3**, 3963 (2009)
11. G. Eda, Y.Y. Lin, C. Mattevi, H. Yamaguchi, H.A. Chen, I.-S. Chen, C.-W. Chen, M. Chhowalla, Adv. Mater. **22**, 505 (2010)
12. H.K. Jeong, M.H. Jin, K.P. So, S.C. Lim, Y.H. Lee, J. Phys. D, Appl. Phys. **42**, 065418 (2009)

13. S. Saxena, T.A. Tyson, E. Negusse, J. Phys. Chem. Lett. **1**, 3433 (2010)
14. S. Shukla, S. Saxena, Appl. Phys. Lett. **98**, 073104 (2011)
15. C. Zhu, S. Guo, Y. Fang, S. Dong, ACS Nano **4**, 2429 (2010)
16. J. Gao, F. Liu, Y. Liu, N. Ma, Z. Wang, X. Zhang, Chem. Mater. **22**, 2213 (2010)
17. K. Karthikeyan, R. Mohan, S.-J. Kim, Appl. Phys. Lett. **98**, 244101 (2011)
18. K.S. Vasu, B. Chakraborty, S. Sampath, A.K. Sood, Solid State Commun. **150**, 1295 (2010)
19. L. Zhang, J. Liang, Y. Huang, Y. Ma, Y. Wang, Y. Chen, Carbon **47**, 3365 (2009)
20. J. Robertson, Mater. Sci. Eng. R **37**, 129 (2002)
21. L. Zhang, X. Li, Y. Huang, Y. Ma, X. Wan, Y. Chen, Carbon **48**, 2367 (2010)
22. E.C. Salas, Z. Sun, A. Luttge, J.M. Tour, ACS Nano **4**, 4852 (2010)
23. J. Zhang, H. Yang, G. Shen, P. Cheng, J. Zhang, S. Guo, Chem. Commun. **46**, 1112 (2010)
24. A. Lerf, H. He, M. Forster, J. Klinowski, J. Phys. Chem. B **102**, 4477 (1998)
25. G. Eda, M. Chhowalla, Adv. Mater. **22**, 2392 (2010)
26. S. Stankovich, D.A. Dikin, R.D. Piner, K.A. Kohlhaas, A. Kleinhammes, Y. Jia, Y. Wu, S.T. Nguyen, R.S. Ruoff, Carbon **45**, 1558 (2007)
27. M. Baraket, S.G. Walton, Z. Wei, E.H. Lock, J.T. Robinson, P. Sheehan, Carbon **48**, 3382 (2010)
28. V.C. Tung, M.J. Allen, Y. Yang, R.B. Kaner, Nat. Nanotechnol. **4**, 25 (2009)
29. I.K. Moon, J. Lee, R.S. Ruoff, H. Lee, Nat. Commun. **1**, 1 (2010)
30. C. Mattevi, G. Eda, S. Agnoli, S. Miller, K.A. Mkhoyan, O. Celik, D. Mastrogiovanni, G. Granozzi, E. Garfunkel, M. Chhowalla, Adv. Funct. Mater. **19**, 1 (2009)
31. F. Tuinstra, J.L. Koenig, J. Chem. Phys. **53**, 1126 (1970)
32. K.N. Kudin, B. Ozbas, H.C. Schniepp, R.K. Prudhomme, I.A. Aksay, R. Car, Nano Lett. **8**, 36 (2007)
33. F. Bonaccorso, Z. Sun, T. Hasan, A.C. Ferrari, Nat. Photonics **4**, 611 (2010)
34. Z. Luo, P.M. Vora, E.J. Mele, A.T.C. Johnson, J.M. Kikkawa, Appl. Phys. Lett. **94**, 111909 (2009)